Published in "Soft Matter 7(17): 7643-7654, 2011"
which should be cited to refer to this work.

Interfacial properties of fractal and spherical whey protein aggregates†

Najet Mahmoudi,*[a] Monique A. V. Axelos[b] and Alain Riaublanc[b]

Fractal and spherical aggregates of whey globular proteins are formed under conditions that coupled heating and shear flow in a plate heat-exchanger at high temperature and for short holding time. Their properties upon adsorption and spreading at the air–water interface have been studied at neutral pH and two subphase conditions. The surface activity of mixtures of aggregates and residual proteins is enhanced and the adsorption behaviour depends strongly on the denatured native-like monomers and the charge screening. After long hours of adsorption, they form a weakly dissipative viscoelastic network, with strong interactions. When spread at the air–water interface, protein aggregates dissociate and form monolayers whose properties are described by scaling laws in the semi-dilute regime. The scaling exponents found in charge-screening subphase conditions correspond to values for polymer in θ-conditions, whereas the values determined in long-range repulsion subphase conditions are intermediate between an ideal (θ-conditions) chain and a chain in good solvent.

Introduction

Due to their amphiphilic nature, whey globular proteins are frequently used as emulsifiers and foam stabilizers.[1,2] The interfacial behaviour of pure β-lactoglobulin, α-lactalbumin and bovine serum albumin, at the air–water and oil–water interfaces has been the subject of extensive research.[3–6] These and other studies have given information on the physicochemical properties that govern the interfacial and rheological properties of whey protein films, and on the correlations that could exist between the interfacial and rheological behaviour of whey proteins and their emulsifying and foaming properties.[7–9]

Because of their high cost of purification, pure β-lactoglobulin, α-lactalbumin and bovine serum albumin are rarely used in food emulsions and foams. Food industry uses rather whey protein concentrates and commercial milk powders as emulsifiers and foam stabilizers.[10,11] However, whey protein concentrates have generally variable protein, salt and sugar compositions, which make their physicochemical and functional properties vary.[12] The variability in composition and functionality of these products comes from differences in the process conditions used in cheese making or casein manufacture, as well as in the manufacture of the whey protein concentrates themselves.[13,14] The processing of whey protein concentrates includes generally an evaporation step that may induce denaturation and aggregation and then modify the protein structure. Since interfacial properties depend strongly on protein structure and bulk conditions such as salt and pH, variations in composition and in degrees of protein structural changes can result in different interfacial and rheological behaviours of whey proteins.[11,15]

Effects of electrostatic interactions on interfacial properties of globular proteins have been studied at the air–water interface. Studies on the effect of protein net charges were based on the kinetic of increase of surface pressure and adsorbed amount for protein solutions at different pH values.[16–19] In these studies, the rate of adsorption and the total adsorbed amount have been found to be highest at pH values close to the isoelectric point where the proteins carry no net charge. Nevertheless, since changing the pH also induces changes in the tertiary and quaternary structures of globular proteins, the pH range that can be investigated to study charge effects on interfacial behavior is limited.[20–22] The alternative approaches were then to chemically modify the net charge of globular proteins[23,24] or to screen the electrostatic charges by increasing the ionic strength.[16–19,23,25] Thus, the protein net charge remains constant while the repulsion energy is lowered, which reduces the contribution from the electrostatic forces to the surface pressure. Increasing the ionic strength was found to result in an increase in the rate of adsorption, the steady-state adsorbed amount and the surface pressure.[18,19,23]

Whey globular proteins are less surface active than the random coil flexible β-casein that adsorbs faster, unfolds and reorients more easily than the ordered β-lactoglobulin and bovine serum albumin.[5,26–28] Upon adsorption at the air–water interface, whey proteins retain their overall globular shape but a partial unfolding is usually observed.[5,29] Irreversible conformational

[a]*Adolphe Merkle Institute, University of Fribourg, Rte Ancienne Papeterie, CP 209, CH-1723 Marly 1, Switzerland. E-mail: najet.mahmoudi@unifr.ch; Fax: +41 26 300 96 24; Tel: +41 26 300 92 58*
[b]*UR 1268 Biopolymères Interactions Assemblages INRA, F-44300 Nantes, France. E-mail: alain.riaublanc@nantes.inra.fr; monique.axelos@nantes.inra.fr*

changes take place during heat-induced interfacial aggregation of a whey protein film heated after two hours of adsorption at the oil–water interface, and enhance the surface activity and the rheological properties.[30] Heat treatment of α-lactalbumin results in partially folded, disulfide bond shuffled states with enhanced surface activity at the air–water interface.[31] Pre-heating β-lactoglobulin was found to result in an increase in surface rheological viscoelasticity because of the decrease in the α-helix content with an increasing flexibility and surface hydrophobicity resulting from the partial unfolding of the molecules.[32] Furthermore, contradictory results were reported on the effect of heat treatment on the surface hydrophobicity of β-lactoglobulin.[32–34] This variability is thought to be related to different heating conditions, which result not only in a partial denaturation of β-lactoglobulin but also in burying patches of high hydrophobicity on protein molecules due to the formation of aggregates.

The issue we concentrate on in this contribution is how aggregation and 3D structure of aggregates of globular whey proteins influence their surface activity and dilatational properties upon adsorption and spreading at the air–water interface.

Materials and methods

Protein aggregates

The whey protein isolate (WPI, 98 wt% protein content) used was purchased from Lactalis Industrie (Laval, France) and is a mixture of 70% of β-lactoglobulin, 20% of α-lactalbumin, 6% of bovine serum albumin and immunoglobulins, and 4% of aggregates due to the spray drying process. To prepare protein solutions a weighed amount of WPI powder was dissolved in milli-Q water containing 0.003 or 0.1 M NaCl at pH 7, under gentle stirring overnight. Protein solutions are subsequently heated in a counter-current plate heat-exchanger. This industrial-like system is composed of three sections where the protein solution is first heated in less than 30 s to the required temperature (80, 100 or 120 °C), then kept at that temperature for a short time (17 to 219 s), and finally cooled down to 20 °C. Protein solutions were sheared in two sections: at 10^2 to 10^3 s^{-1} when heated between the plates at all temperatures, and at 10^5 to 10^6 s^{-1} due to intensive shearing load during cooling only for solutions heated at 100 and 120 °C. Two concentrations were investigated: 3 g L^{-1} at 0.1 M and 15 g L^{-1} at 0.003 M. These concentrations were selected to obtain aggregates of 50–300 nm size. The samples were refrigerated at 4 °C until examination with different techniques.

Bulk characterization of aggregates

To quantify residual native-like proteins which coexist with aggregates, gel filtration chromatography (GFC) experiments were performed on TSK 6000 column SWXL (Tosohaas, Montgomeryville, PA) equilibrated in a 0.05 M Tris solution containing 0.1 M NaCl, using a flow rate of 0.4 mL min^{-1}. This column theoretically separates globular proteins with molecular weight up to 2×10^8 g mol^{-1}. The eluted protein was detected using UV absorption at 280 nm and the amount of residual native-like protein was calculated as % area relative to the area of unheated protein.

The size and the shape of the aggregates were determined using dynamic and static light scattering (DLS, SLS), small-angle neutron scattering (SANS) and cryogenic transmission electron microscopy (cryo-TEM). SLS and DLS measurements were performed using an ALV-5000 multi-bit multi-tau correlator and a Spectra Physics solid state laser operating with vertically polarized light at $\lambda = 532$ nm. The protein solutions were measured in cylindrical scattering vials immersed in a refractive index matching bath of filtered decalin, and the temperature kept at 20 ± 0.1 °C. SLS and DLS experiments were performed at θ ranging from 10 to 140°, corresponding to a q-range of $3.0 \times 10^{-3} \leq q \leq 3.5 \times 10^{-2}$ nm^{-1}

$$q = \frac{4\pi n}{\lambda} \sin\left(\frac{\theta}{2}\right) \quad (1)$$

with the refractive index of the solvent, n. SLS experiments have been analysed using the Guinier approximation to determine particle mass, $\langle M_w \rangle$, and gyration radius, $R_g{}^0$.[35] DLS experiments have been analysed in terms of a distribution of relaxation times using the Laplace inversion routine REPES.[36] SANS measurements were performed on the SANS spectrometer PACE at the Laboratory Léon Brillouin (LLB) in Saclay (France). The protein solutions were characterized over a two-decade q-range, $0.03\ nm^{-1} < q < 3\ nm^{-1}$, using a combination of two wavelengths: $\lambda = 0.5$ nm with a sample-to-detector distance of 1.35 m and $\lambda = 1.2$ nm with a sample-to-detector distance of 4.54 m. Samples were measured in 1 or 2 mm Hellma quartz cells at room temperature. The raw data were corrected for background scattering, detector efficiency, the incident neutron beam, and converted to an absolute cross-section $I(q)/cm^{-1}$ using standard LLB procedures.[37,38]

In heated WPI solutions, H_2O was exchanged using repeated centrifugal filtrations in 10 kDa cutoff Amicons (Amicon, Beverly, MA), and diluting concentrated dispersions with D_2O with 0.003 M or 0.1 M NaCl after each cycle. The native WPI solution was prepared directly in D_2O. Size distributions of aggregates were invariant on solvent exchange.

The q-dependence of the absolute scattering cross-section can be written as

$$I(q) = n_{part}(\rho_{part} - \rho_{solv})^2 V_{part}{}^2 P(q) S(q) \quad (2)$$

with the particle number density, n_{part}/cm^{-3}, the particle coherent scattering length density, ρ_{part}/cm^{-2}, the solvent coherent scattering length density, ρ_{solv}/cm^{-2}, the particle volume, V_{part}/cm^3, the form factor, $P(q)$, and the structure factor, $S(q)$.

Cryo-TEM micrographs were taken at 95 K on a JEM-1230 'cryo' microscope (Jeol, Japan) operating at 80 kV. Protein solutions were deposited onto glow-discharged holey-type carbon-coated grids (Ted Pella Inc., USA), vitrified using liquid ethane and imaged under low dose conditions (<10 electrons $Å^{-2}$). A detailed description of the techniques used to characterize the molecular characteristics, structure and morphology of aggregates (SLS, DLS, SANS and cryo-TEM) is given in ref. 39.

In addition to the 3D-structure of aggregates, we looked at changes in secondary structure of proteins induced by heating. We used Attenuated Total Reflection Fourier Transform Infra-Red (ATR-FTIR) spectroscopy (see details about the technique and results in the ESI†).

Interfacial characterization of aggregates

The kinetics of surface tension decrease and the dilatational properties were measured using a dynamic drop tensiometer (Tracker, I.T. Concept, France), see description in ref. 40. A 6 μL air bubble was formed upward at the tip of a U-shaped stainless steel needle immersed in a cuvette filled with the protein solution at 0.5 g L^{-1}, both of which are thermostatted at 20 ± 0.1 °C. The tension decrease was followed using axisymmetric drop-shape analysis. Image acquisition and regression of the interfacial tension were performed with Windrop software by fitting the Laplace equation to the drop shape. Windrop software also controlled an automatic pipetting system that maintained constant drop volume over the long time periods of measurement. The interfacial dilatational moduli were measured by varying periodically the interfacial area of 6.25%, at frequency from 0.0025 to 0.1 Hz. The dilatational modulus was determined at the end of the adsorption. It is related to the changes in the interfacial tension, $\Delta\gamma$, and the interfacial area, ΔA, by:

$$\varepsilon = A(\Delta\gamma/\Delta A) \tag{3}$$

The elastic dilatational modulus ε' and the viscous dilatational modulus ε'' were calculated from ε and the phase angle between the changes in interfacial tension and area, Φ, by:

$$\varepsilon' = \varepsilon\cos\,\Phi \tag{4}$$

$$\varepsilon'' = \omega\eta_d = \varepsilon\sin\,\Phi \tag{5}$$

with the frequency of compression/expansion, ω, and the interfacial dilatational viscosity, η_d.

Surface pressure *vs.* area (Π–A) isotherms were recorded using a two-symmetrical barrier Langmuir trough with a filter paper Wilhelmy plate sensor (Nima Technology, UK). The PTFE trough, with an area of 70 × 10 cm^2, was filled with approximately 500 mL of salt solutions and the impurities removed from the surface. Solutions of WPI aggregates, typically 50 μL of 1 g L^{-1}, were spread under dilute conditions or at very low pressures (≤0.5 mN m^{-1}), dropwise using a microsyringe. The temperature of the subphase was held at 20 °C by a controlled-temperature water circulation. The spread layer was left for at least 30 min to reach equilibrium, and then compressed at 40 cm^2 min^{-1}. The surface pressure Π_{eq} is then recorded as a function of surface area of the protein spread at the interface. Dilatational properties of protein monolayers were derived from the equilibrium surface pressure–area isotherms. Film elasticity of protein monolayers at zero deformation rate, ε_{eq}, can be calculated from the slope of the Π–A isotherm:

$$\varepsilon_{eq} = -A\partial\Pi_{eq}/\partial A \tag{6}$$

Protein films at different pressures are transferred at a speed of 0.1 mm s^{-1} onto freshly cleaved mica plates, using the Langmuir–Blodgett technique. The structure of the transferred films was imaged using an AFM East Coast Scientific (ECS, Ltd., Cambridge, UK) and performed in contact mode, in butanol and under ambient conditions, using a 10 × 10 μm^2 scanner. Topographic images were acquired in constant force mode using silicon nitride tips on integral cantilevers.

Results

Molecular characteristics of heated WPI

Fig. 1 shows a set of gel filtration chromatograms of WPI (15 g L^{-1}, 0.003 M, pH 7) heated at 80, 100 or 120 °C. Heating solutions of whey proteins to temperatures above the denaturation temperature of major proteins, β-lactoglobulin[41] and α-lactalbumin,[42] for less than 3 minutes results in a decrease of the broad "native" peak and the formation of a new peak corresponding to aggregates. Additionally, the intensity of this peak increases with rising temperature. Indeed, heating at 80 °C induces the formation of a low fraction of aggregates, while heating at higher temperature results in shifting the aggregates' peak to higher molecular weight and its broadening. Similar chromatographs were obtained for a WPI at 0.1 M and 3 g L^{-1}. Quantitative analysis of the chromatographs allowed for the determination of the fraction of residual native-like proteins.

In Table 1 are summarized the residual fraction of non-aggregated major proteins, β-lactoglobulin and α-lactalbumin, as a function of heating temperature. This residual fraction drops from 76% at 80 °C to 18% at 120 °C in a 15 g L^{-1} solution at 0.003 M after 145 s of heating, compared to a decrease from 66% to 5% in a 3 g L^{-1} solution at 0.1 M. A high salt concentration then promotes aggregation more efficiently than a high protein concentration (protein counterions increase the ionic strength as 0.33×10^{-3} C (g L^{-1})). Adding salt shrinks the Debye double layer, screening the electrostatic repulsion between the protein molecules until they aggregate.

Molecular characteristics of aggregates, such as aggregate size and mass, were obtained from DLS and SLS experiments, as reported in Table 1. Comparing values obtained by Guinier approximation, we found that the aggregate mass increases exponentially with temperature for both ionic strengths. This increase is slightly steeper at low ionic strength. Similarly to the aggregate mass, the gyration radius grows exponentially but

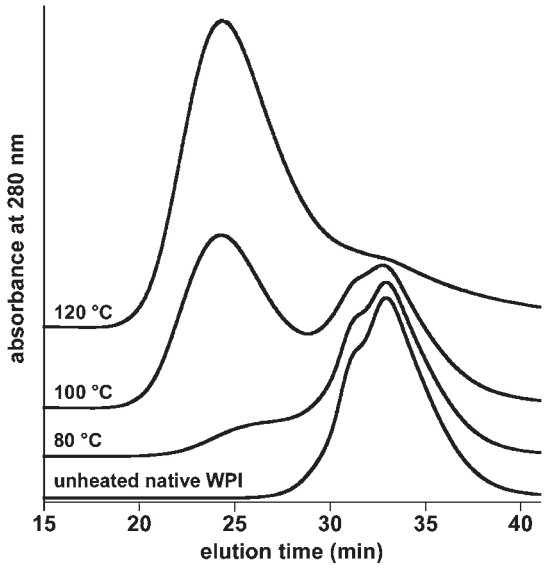

Fig. 1 GFC chromatograms for native and heat-treated whey protein isolate (3 g L^{-1}, 0.003 M NaCl, pH 7) in a plate heat-exchanger for 145 s at 80, 100 and 120 °C. The curves are offset for clarity.

Table 1 Residual fraction of major whey proteins (β-lactoglobulin + α-lactalbumin) and molecular characteristics of native WPI and WPI aggregates formed at 0.003 M and 1.5 wt% or 0.1 M and 0.3 wt% and heated at various temperatures for 145 s. Experimental error in light scattering experiments is estimated at around 10–15%. R per nm, M_w per kg mol^{-1}

I/M	T/°C	Residual fraction (F)[a]	M_w[b]	R_g[b]	R_h^0[d]	R_g/R_h^0
0.003	20	90	26.7	2.42[c]	2.3	1.05
0.1	20	90	44.3	4.02[c]	3	1.34
0.003	80	76	1838	35.7	29.8	1.2
	100	54	28 205	48.2	54.5	0.88
	120	18	288 150	78.3	81.1	0.97
0.1	80	66	3957	55.1	46.2	1.2
	100	21	42 245	105.3	162.2	0.65
	120	5	172 340	119.1	161.5	0.74

[a] From GFC. [b] Guinier approximation of SLS data. [c] From SANS experiments. [d] REPES analysis of DLS data.

weakly with temperature. However, the aggregates formed at high ionic strength are almost twice as large in size compared to the aggregates formed at low ionic strength. Values of R_g/R_h (R_h, hydrodynamic radius) decrease from 1.2 to 0.65 with increasing temperature ($R_g/R_h = 0.775$ for uniform hard spheres). High ratio close to the value found at 80 °C has been reported for β-lactoglobulin aggregates obtained after heating at 70 or 76 °C.[43]

Cryo-TEM and SANS experiments have been performed to elucidate the shape and structure of WPI aggregates. Fig. 2 shows cryo-TEM images of aggregates formed at 1.5 wt% and 0.003 M, or 0.3 wt% and 0.1 M; and heated at 80, 100 or 120 °C. Qualitatively, it can be seen that aggregates formed at 80 °C have a rather irregular shape and appear, at least at low ionic strength, as an ensemble of individual and assembled thin curved strands. All of the aggregates formed at higher temperature were observed to be roughly spherical, individual at low ionic strength whereas loosely bound at high ionic strength. The average and standard deviation of the particle diameters on several images (50 to 100 particles identified) were calculated, the polydispersity determined as the ratio of the standard deviation and the average particle size. The average diameter of aggregates formed at low ionic strength was $\langle 2R \rangle = 88 \pm 26$ nm compared to a $\langle 2R_h^0 \rangle = 109$ nm at 100 °C, and $\langle 2R \rangle = 134 \pm 43$ nm compared to a $\langle 2R_h^0 \rangle = 162$ nm at 120 °C. Aggregates formed at higher ionic strength are larger, $\langle 2R \rangle = 187 \pm 46$ nm compared to a $\langle 2R_h^0 \rangle = 324$ nm at 100 °C, and $\langle 2R \rangle = 253 \pm 66$ nm compared to a $\langle 2R_h^0 \rangle = 323$ nm at 120 °C. Except for the aggregates formed at 100 °C and 100 mM, all particle sizes determined from microscopy are close to twice the hydrodynamic radius determined with DLS.

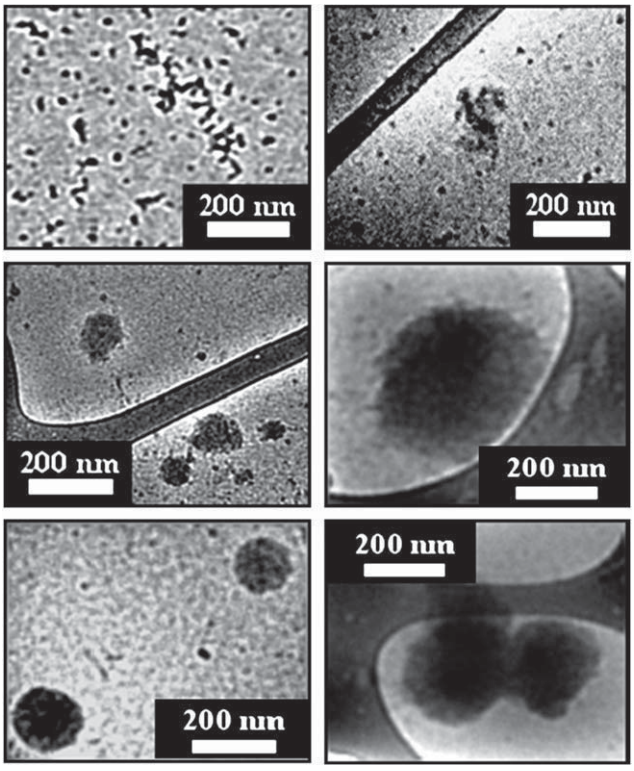

Fig. 2 Cryo-TEM micrographs of WPI aggregates heated for 145 s, at 0.003 M and 15 g L^{-1} (left images) or at 0.1 M and 3 g L^{-1} (right images) at 80, 100 °C or 120 °C (from top to bottom).

SANS experiments have been performed to determine the WPI form factor and the structure of WPI aggregates, strand-shaped formed at 80 °C and spherical-like formed at 120 °C. The scattering from native WPI at neutral pH (Fig. 3) is adequately described by that of a sum of two attached spheres representing a dimer of β-lactoglobulin with a radius of 1.55 nm, a single sphere of 1.45 nm of radius representing α-lactalbumin, and a prolate ellipsoid representing bovine serum albumin with dimensions of semi-axes of 7 and 2 nm, using ratios given in Materials and methods section above.[43–46] At $q < 0.2$ nm^{-1}, the scattering shows an upturn due to the presence of small aggregates that is accounted for using a mass fractal with a radius of 30 nm. Due to the coexistence of aggregates and native-like proteins, the scattering intensity from heated solutions was fitted using the two contributions. Indeed, scattering from solutions heated at 80 °C was modelled using the form factor of polydisperse spheres (20%) of 1.4 nm to account for residual native-like proteins, and a mass fractal structure factor of polydisperse spheres (12%) of 1.55 nm (as elementary units or monomers) to describe aggregates (Fig. 3). The fractal dimension and gyration radius obtained are respectively 2.19 and 25.9 nm at 0.003 M and 2.15 and 43 nm at 0.1 M. The R_g values are nevertheless smaller than the values determined using SLS. The fractal dimension values obtained agree well with typical values for reaction limited cluster aggregation (RLCA).[47] SANS scattering curves of aggregates formed at 120 °C confirm their spherical morphology. Indeed, the experimental data (Fig. 3) are well described by

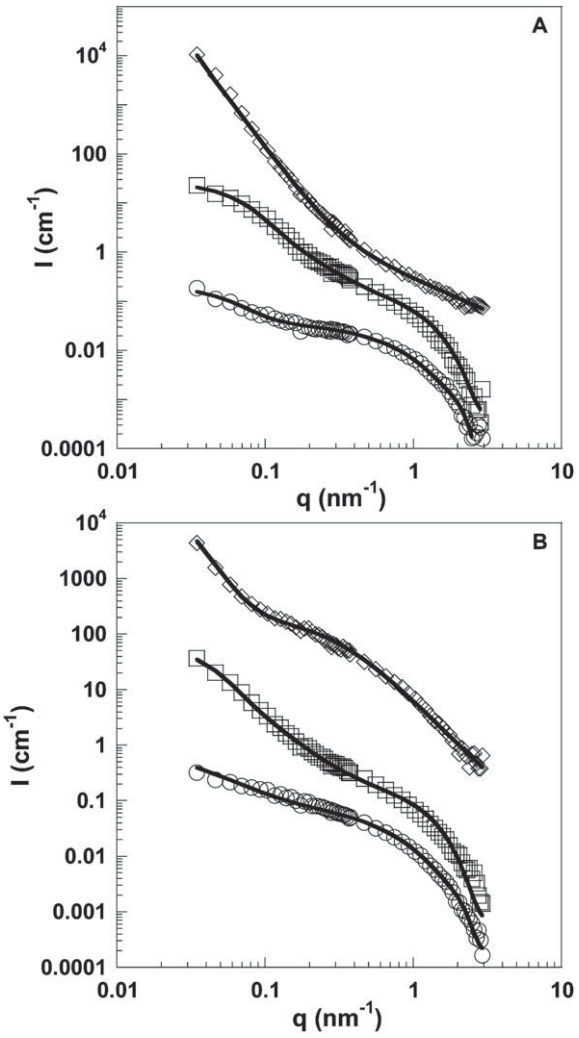

Fig. 3 SANS scattering curves from native WPI (○), WPI aggregates heated for 145 s in a plate heat-exchanger at 80 °C (□) or 120 °C (◇) at 0.003 M and 15 g L^{-1} (A) or 3 g L^{-1} and 0.1 M (B). Open symbols correspond to experimental data; solid lines represent fits with a sum of different models as explained in the text for native WPI, with polydisperse mass fractal aggregates for WPI at 80 °C, and with a polydisperse sphere for WPI heated at 120 °C. The curves are shifted vertically for better visibility.

a model for polydisperse sphere, with an internal fractal structure. The scattering curve from spherical aggregates formed at low ionic strength was modelled using a polydisperse sphere (39% polydispersity) of 96 nm radius and an internal structure with fractal dimension of 1.3. For a homogeneous scattering sphere, the radius of gyration is calculated as $R_g = 0.775$ R, and equals 74.4 nm which is very close from the value determined by Guinier approximation of SLS data (78.3 nm). The scattering curve showed no visible peak or shoulder at high q-values, contrary to the scattering curve from spherical aggregates formed at high ionic strength. Indeed, the experimental scattering data from spherical aggregates formed at high ionic strength were described fairly well using a polydisperse sphere (26% polydispersity) of 124 nm of radius with a mass fractal internal structure of $D = 2.48$ and 6.5 nm of radius. The radius of gyration calculated equals to 96.1 nm, smaller than the value found by Guinier approximation of SLS data (119 nm). The polydispersity of the spherical aggregates determined from SANS is very similar to the polydispersity measured from cryo-TEM, 39% *versus* 32.2% at low ionic strength and 26 *versus* 26.1% at high ionic strength.

Adsorption and dilatational rheological properties

In Fig. 4A and 5A, we report the increase of surface pressure at the air–water interface for native and aggregated WPI at 0.5 g L^{-1} and pH 7, 0.003 M and 0.1 M respectively. Almost all curves show three regimes: the surface pressure first increases steeply at short times (first decade), then it almost flattens but keeps increasing very weakly (over almost two decades), and finally it resumes increasing. These three regimes of surface pressure increase are usually and respectively attributed to adsorption of proteins to the surface of the air bubble, to saturation and

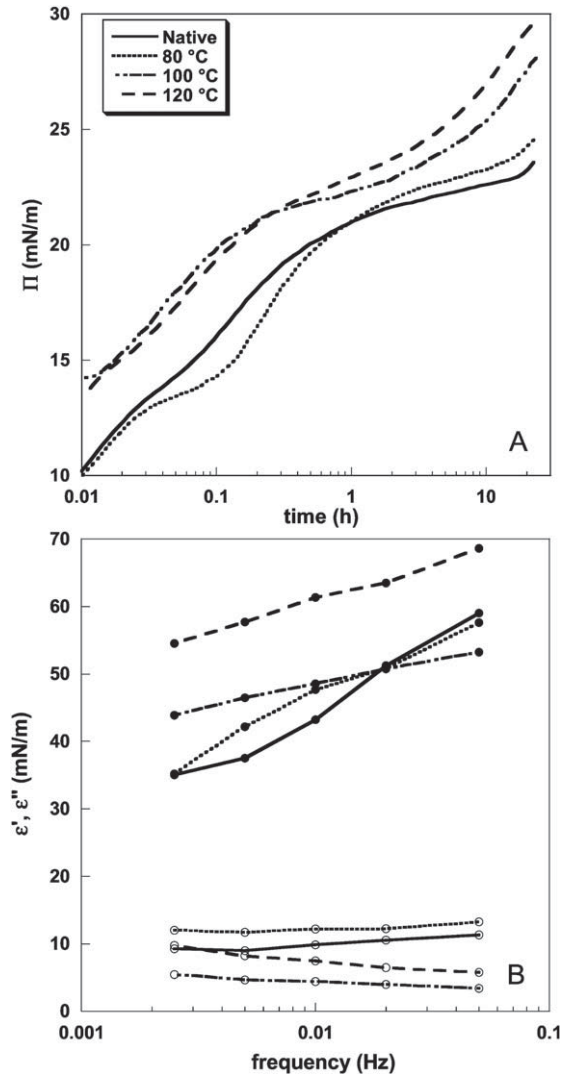

Fig. 4 Effect of protein heating temperature on kinetic of surface pressure increase at air/water interface (0.5 g L^{-1} at pH 7 and 0.003 M) (A), and on the dilatational frequency sweep after 24 h of adsorption, ε' (filled symbols) and ε'' (open symbols) (B).

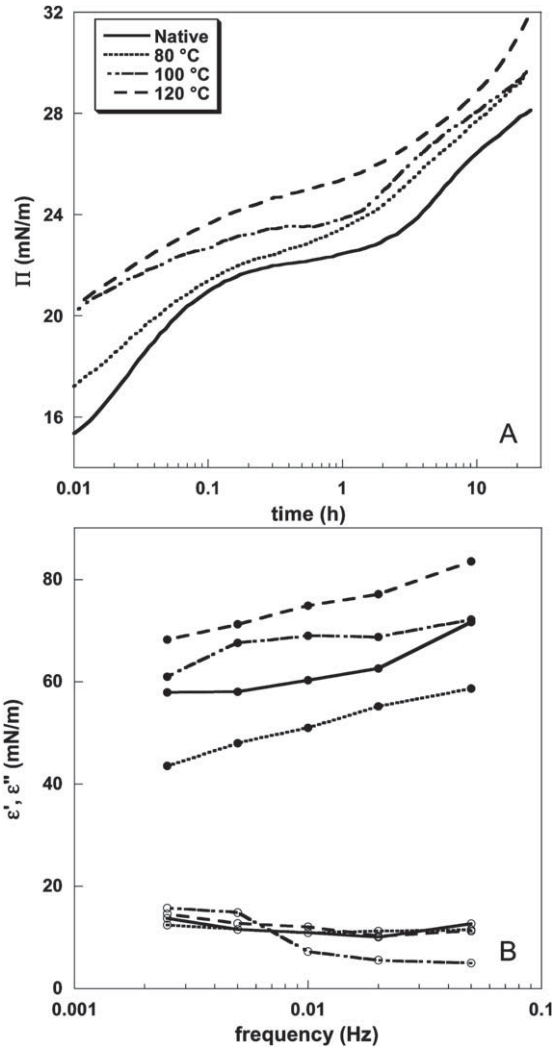

Fig. 5 Effect of protein heating temperature on kinetic of surface pressure increase at air/water interface (0.5 g L^{-1} at pH 7 and 0.1 M) (A), and on the dilatational frequency sweep after 24 h of adsorption, ε' (filled symbols) and ε'' (open symbols) (B).

conformational changes, and to continuous conformational rearrangements within the film and/or to multilayer formation.[48–50] The induction regime usually observed for globular proteins was not observed because of the high protein concentration investigated.[51] At both ionic strengths, all of the heated WPI were observed to have faster adsorption kinetics compared to native WPI. Additionally, the adsorption kinetic becomes faster with increasing heating temperature. Nevertheless, when comparing native or heated proteins in different ionic strengths, proteins at high ionic strength increase more rapidly the surface pressure compared to low ionic strength's systems. This faster behaviour is the consequence of reducing the electrostatic repulsions that lowers the energy barrier generally formed by the first protein molecules anchored at the interface and then accelerates the adsorption.

The second set of experiments on drop tensiometer was aimed at determining the dilatational rheological properties of protein films. Fig. 4B and 5B show frequency sweeps after 24 h of adsorption, assuming that the layer is almost in equilibrium since the pressure increase was substantially lowered. For systems at low ionic strength, the dilatational storage modulus of native and aggregated proteins is approximately an order of magnitude larger than the loss modulus, suggesting that the interface is a weakly dissipative viscoelastic system. Additionally, the loss modulus decreases monotonically for the 100 and 120 °C systems while it increases monotonically for the native and the 80 °C systems. This implies that the native WPI and the 80 °C's mixture of 74% residual proteins and fractal aggregates formed fluidlike layers that continue to relax even at very short time-scale (20 s), while the 100 and 120 °C's mixtures of lower fractions of residual proteins and larger aggregates formed solidlike layers in which relaxations take place at longer times (400 s). For systems at high ionic strength, the dilatational storage modulus is at least five times higher than the loss modulus, implying that the protein layer behaves as also as a weakly dissipative viscoelastic system in this frequency range. The 100 and 120 °C's aggregate films are more elastic than the native WPI and the 80 °C's aggregate films. In addition, more relaxations take place in the films of WPI heated at 80 °C and native WPI than in the films of WPI heated at 100 and 120 °C.

Spreading behaviour and film elasticity

Aggregates formed in electrostatic-repulsion conditions. The surface pressure isotherms displayed good reproducibility, and the irreversible loss of film material upon repeated compression/expansion cycling was very limited, even for the very large aggregates. We have chosen here to show the compression isotherms only. Spread whey protein monolayers were characterized by recording the surface pressure (Π)–surface area (A) isotherms, then converted into Π–Γ (interfacial protein concentration) curves assuming no protein loss in the subphase on spreading. The results of native and heated WPI are shown in Fig. 6A. At the very early stages of compression corresponding to low surface concentrations, the surface pressure is very low defining the dilute regime.[52] As the surface area is reduced, the pressure increases, resulting from the proteins and/or the aggregates at the surface coming into contact with each other. This first increase defines the semi-dilute regime.[52] The surface pressure continues to increase as a consequence of increasing the surface concentration of the native WPI molecules and/or the heat-induced aggregates, and converges to the same concentrated regime. The isotherms of the three heated solutions are shifted to higher concentrations compared to the unheated protein isotherm. This shift is temperature dependent and we can suppose that it is residual fraction dependent. However, by plotting the pressure *versus* the surface "non-aggregated protein concentration" (Fig. 6B), the curves do not superimpose and are rather shifted to lower concentrations compared to the native WPI isotherm. This suggests that it is not only the residual non-aggregated proteins but also the aggregates that contribute to the formation of the interfacial layer.

The increase of pressure for all the films scales as a power law of the surface concentration, $\Pi \propto \Gamma^{\nu}$, in the semi-dilute regime.[53] The scaling exponent is 6.2, 6 and 4.2 respectively for the 80, 100 and 120 °C's mixtures of residual and aggregated proteins, compared to 5.5 for the native WPI. In addition, for the 100 and

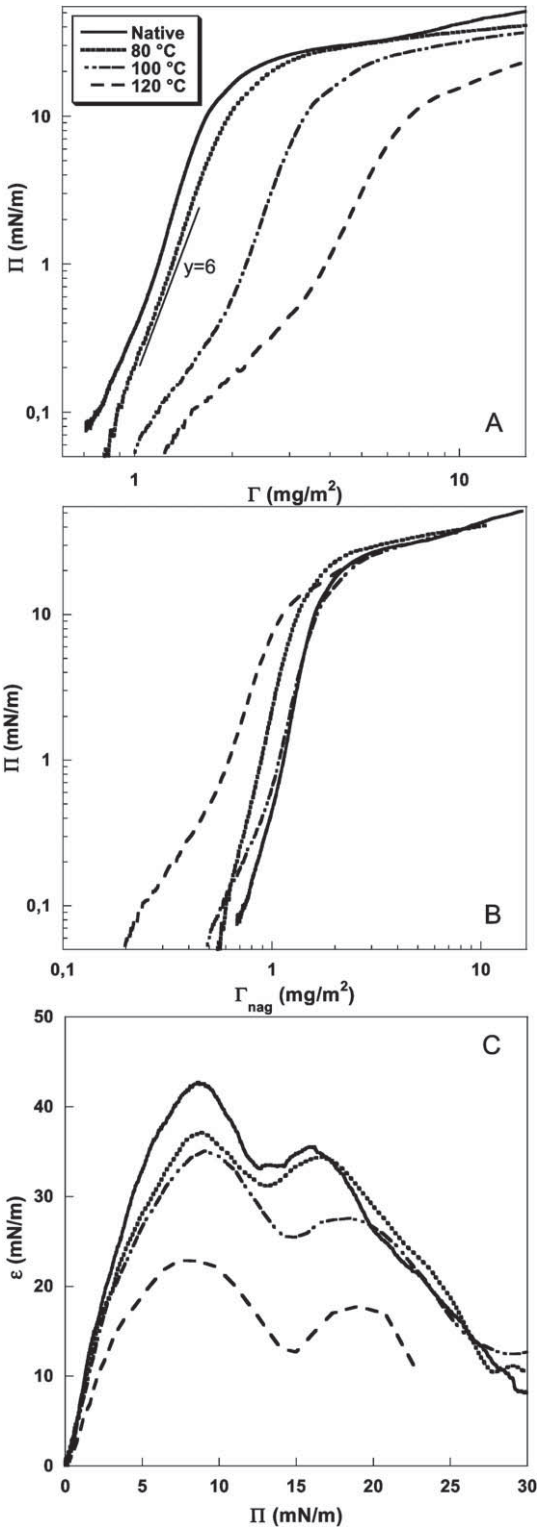

Fig. 6 Effect of heating temperature on Π–Γ isotherms (A), on Π–Γ isotherms corresponding to the residual fraction (B) and on dilatational modulus as a function of pressure (C), corresponding to the WPI aggregates (pH 7, 0.003) spread on 0.003 M subphase.

120 °C systems, a second power law region can be seen at low pressure ($\Pi < 0.5$ mN m^{-1}). This sort of lag-phase, which cannot be considered as the dilute regime, has also been observed for large aggregates prepared in static conditions.[54] In Fig. 6C are presented the elasticity curves calculated from the isotherms. They all show two peaks at 8–9 mN m^{-1} and 17–19 mN m^{-1}. The maximum elasticity peak values decrease with the heat-treatment and the residual fraction of proteins, suggesting that the aggregates contribute a little to the formation and the elasticity of the layers at 0.003 M.

By spreading the solutions on a 0.1 M subphase and then screening the lateral electrostatic repulsions between the residual and aggregated proteins, all the isotherms shift to lower surface concentrations (Fig. 7A). While the 80 and 100 °C systems' isotherms shift close to the native WPI isotherm, the 120 °C system's isotherm remains at relatively high surface concentrations. This suggests that the aggregates become rigid with increasing temperature which makes them less susceptible to rearrangements at the interface. In addition, the lag-phase already observed in the presence of electrostatic repulsions remains in conditions of screening charges. The behaviour of the 120 °C's aggregates at low surface pressure is different from that

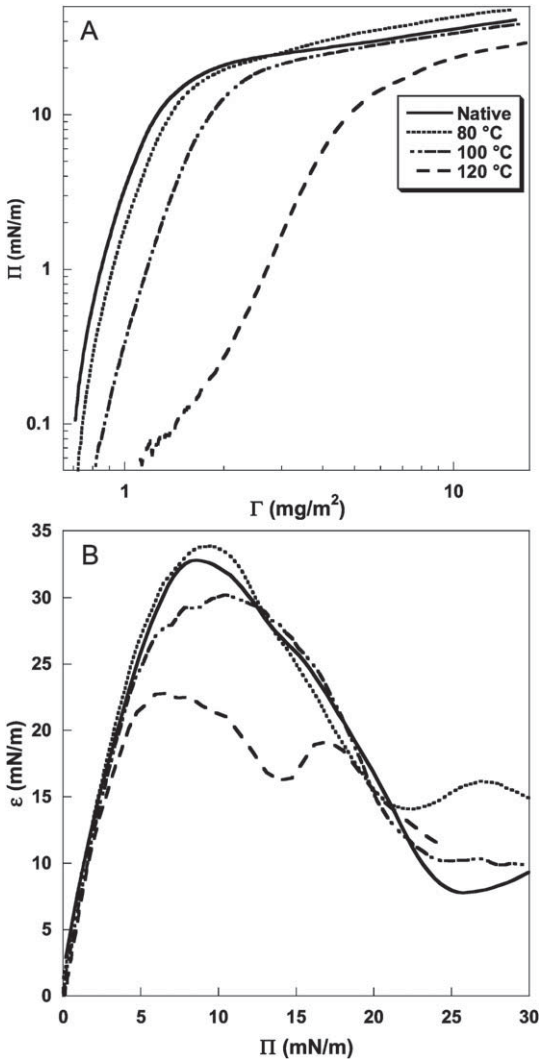

Fig. 7 Effect of heating temperature on Π–Γ isotherms (A), and on compression modulus as a function of pressure (B) of the WPI aggregates (pH 7, 0.003 M) spread on 0.1 M subphase.

of the native WPI, 80 and 100 °C's aggregates. The surface pressure increases very sharply at these early stages of compression which makes the semi-dilute regime short. The power-law scaling exponents of surface pressure *vs.* surface concentration in the semi-dilute regime are found to be larger in charge screening conditions. Indeed, they decrease from 8.3 at 80 °C, to 7 at 100 °C, and to 4.7 at 120 °C, compared to 7.5 for native WPI. Comparing these exponents to those found on a salt-free subphase underlines the compact structure of the aggregates especially at 80 and 100 °C and suggests that screening the lateral charge repulsions between molecules decreases the swelling effect of the double ionic layer.[53] The particular behaviour of the layer formed by the 120 °C's mixture is confirmed in the elasticity curves on which two distinct peaks at 7 and 17 mN m^{-1} are shown (Fig. 7B). Distinctly from this system, solutions heated at 80 and 100 °C show a single peak at Π around 10–11 mN m^{-1} with elasticity values larger than the 120 °C's first peak value and slightly lower than the maximum elasticity of the native WPI film.

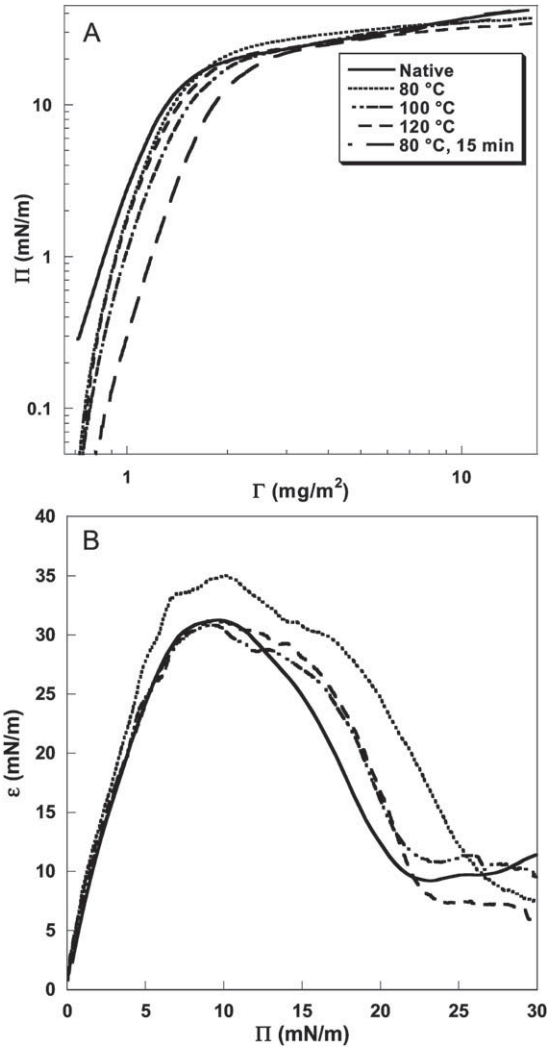

Fig. 8 Effect of heating temperature on interfacial behaviour of WPI aggregates (pH 7, 0.1 M) spread on 0.1 M subphase: (A) Π–Γ isotherms and (B) elasticity dependence on the pressure.

Aggregates formed in charge-screening conditions. Fig. 8A shows the results of the native WPI and aggregates prepared and spread on a 0.1 M solution at neutral pH. All isotherms of mixtures of residual and aggregated proteins superimpose over the whole surface concentration range and are only slightly shifted to higher concentrations compared to the native WPI isotherm. This similar behaviour of the native WPI and mixtures of various residual non-aggregated and aggregated fractions suggests that the aggregates disassemble and rearrange at the air–water interface and form layers rather similar to the native whey protein layer. As already observed for the native WPI, 80 and 100 °C's aggregates prepared in 0.003 M and spread on a 0.1 M subphase, the surface pressure of all the aggregates prepared and spread in the presence 0.1 M increases very sharply at the very early stages of compression though the first pressure values are very low ($\Pi < 0.1$ mN m^{-1}). This stage corresponds to the dilute regime where the pressure increases linearly with the surface concentration if the system is in equilibrium. This steep increase suggests that the aggregates do not reach equilibrium 30 min after they are deposited. For all these heated systems, a limited power-law scaling is found in the semi-dilute regime. The scaling exponent found was 8.5, higher than the value of native WPI $y = 7.1$. This difference can be attributed to a more compact structure in the interfacial films of the heated solutions.[53] The elasticity curves of films formed by the 0.1 M NaCl native and aggregated WPI show all a maximum of 30 mN m^{-1} at 8–9 mN m^{-1} followed by a shoulder at 15 mN m^{-1} (Fig. 8B). The maximum has been associated with the onset of a conformational change in the monolayer of proteins.[26]

When deposited on a 0.003 M subphase, the native and aggregated proteins spread less due to strong lateral electrostatic repulsion that shifts the onset of pressure increase to higher concentrations and prevents protein molecules from forming close-packing layer at lower concentration (Fig. 9A). Furthermore, solutions at 80 and 120 °C behave very similarly to native WPI whereas the isotherm of solution at 100 °C shifted to larger concentration. In the semi-dilute regime, all the systems show a power low scaling, with very similar exponents (5.7, 6.3, 5.8 and 5.6 for native WPI, 80, 100 and 120 °C, respectively).

The corresponding equilibrium moduli derived from Π–Γ isotherms are presented in Fig. 9B. They all show two peaks at $\Pi \approx 9$ and $\Pi \approx 15$ mN m^{-1}. The first peak value decreases from 37 mN m^{-1} for native WPI to 30 mN m^{-1} for WPI at 100 and 120 °C, whereas the second peak is constant at 28 mN m^{-1}.

Film structure

Fig. 10 shows topographical images of spread native WPI monolayer transferred at a surface pressure of 15 mN m^{-1} and aggregated WPI layers transferred at 12 mN m^{-1}. The native WPI monolayer shows a grainy structure with a relatively homogeneous background of average roughness of 0.6 nm and containing few aggregates of 3–5 nm height and 30–50 nm large. These aggregates have already been identified in SANS experiments on native WPI. The topographical images of layers of whey protein aggregates prepared and spread on a 0.003 M subphase, at 12 mN m^{-1}, show interfacial structures composed of close-packed small assemblies of whey proteins. The mean size of these assemblies increases with the heating temperature of the

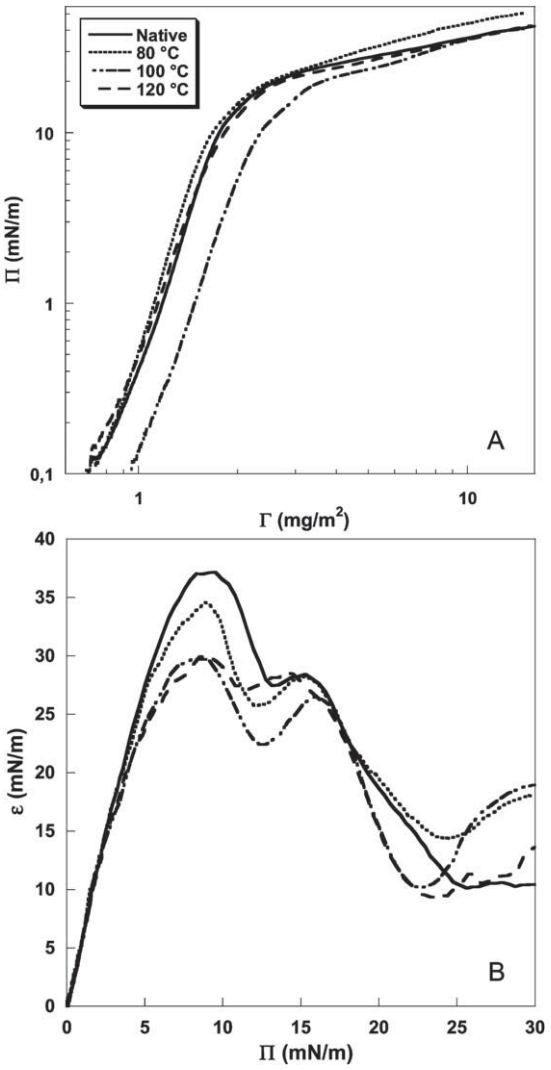

Fig. 9 Effect of heating temperature on interfacial behaviour of WPI aggregates (pH 7, 0.1 M) spread on 0.003 M subphase: (A) *Π–Γ* isotherms and (B) elasticity dependence on the pressure.

aggregates. For the system heated at 80 °C, the film mainly composed of native-like proteins shows assemblies of a mean diameter of 15 nm, while at 100 and 120 °C the mean diameter is respectively 21 and 30 nm. A measured mean height of some 5 nm is about the same for all the aggregates and is higher than the thickness of the native WPI's film.

The images of films of solutions heated at high ionic strength (Fig. 11) show heterogeneous structures with a relatively uniform background of close-packed objects of 12 nm of diameter and 0.5 nm of roughness, and a few larger objects with 50 nm of diameter and protruding of 2–3 nm. Similar AFM images were recorded for spread β-lactoglobulin monolayers at a surface pressure of 12.6 mN m^{-1}, with lower roughness of the films compared to the values mentioned above suggesting a thickening effect of the aggregates on the films.[55]

Discussion

Protein aggregates were shown to shift from fractal structures at low temperature to spherical particles at higher temperature.

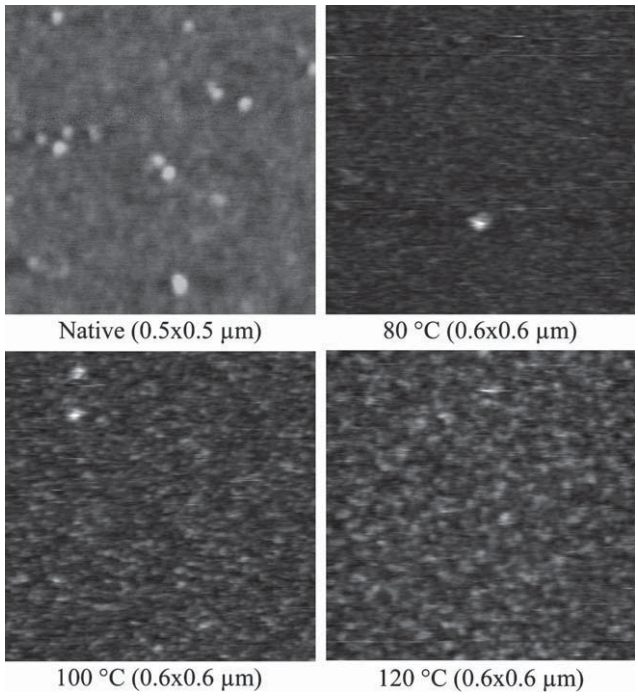

Fig. 10 AFM topographical images of Langmuir–Blodgett films of spread 0.003 M native WPI at 15 mN m^{-1} and aggregated WPI at 12 mN m^{-1} (0.003 M subphase).

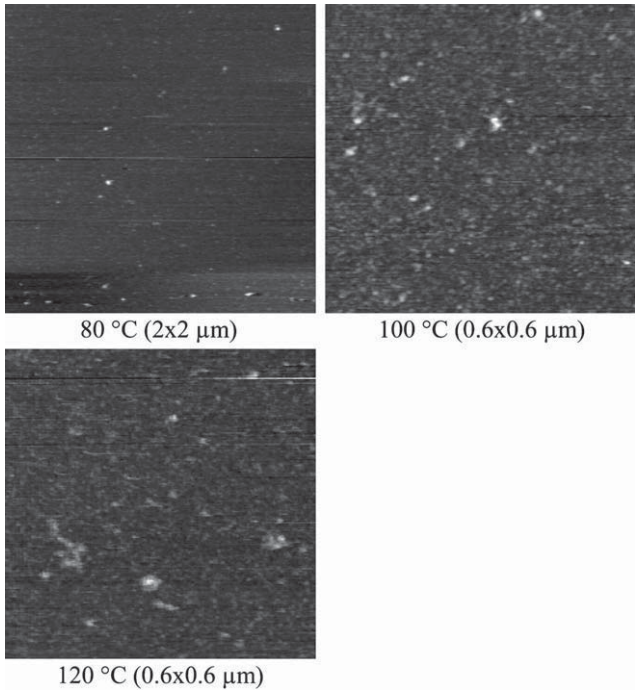

Fig. 11 AFM topographical images of Langmuir–Blodgett films of 0.1 M NaCl WPI aggregates at 12 mN m^{-1} (0.003 M subphase).

This transition in structure has been proposed to be thermodynamically driven by a decrease in the activation energy of the denaturation of β-lactoglobulin with increasing temperature. Both fractal and spherical aggregations were driven by medium to short-range repulsion and hydrophobic non-covalent

attraction. Details on mechanisms of structure formation and interactions stabilising these aggregates are discussed elsewhere.[39] In this section, we discuss the adsorption and spreading behaviour of heated whey protein solutions, the viscoelasticity and structure of films they form at air–water interface.

Adsorption behaviour

For all the systems studied, increasing the ionic strength resulted in an increase in the rate of adsorption and the "equilibrium" surface pressure, which resulted from the screening of the electrostatic charges of proteins concentrating at the interface by the sodium and chloride ions and then effectively reducing the contribution of electrostatic repulsions to the surface phenomena. These results confirm the strong effect of the electrostatic interaction on the surface activity of globular whey proteins.[18,19,23]

At the air–water interface, the heated solutions adsorb more rapidly than the native WPI. Since these heated solutions are all mixtures of aggregates and residual non-aggregated proteins, the residual proteins are assumed to be the first molecules to reach the interface because of their higher diffusion coefficient compared to the aggregates which diffuse more slowly to the interface because of their larger size. Additionally, the use of a non-limiting concentration in this study (0.5 g L^{-1}) provides enough residual non-aggregated proteins to saturate the interface since the lowest residual fraction was 5% within the aggregates at 120 °C and 0.1 M, which implies a residual concentration of 0.025 g L^{-1}. It is well known that β-lactoglobulin, which associates mainly as dimer at neutral pH, dissociates into monomers when heated above 60 °C.[56] The dissociation of β-lactoglobulin into monomers is confirmed by SANS data at 80 °C, where the residual native-like proteins were best accounted for using a form factor of spheres of 1.4 nm which corresponds to the value determined for β-lactoglobulin monomer, 1.39 nm.[57] So, assuming that all residual β-lactoglobulin molecules are in the monomeric state, they diffuse more quickly to the interface than the dimers of the native WPI and then adsorb and saturate more efficiently. The adsorption rate (determined from the steep increase of surface pressure at short times) increases with raising the heating temperature of protein solutions. The short-time adsorption can be essentially related to the denatured state of the residual proteins since for the 80 °C mixture, we have determined by micro-Differential Scanning Calorimetry (results not shown) that a large fraction of the residual proteins is not denatured while for the 100 and 120 °C systems, all the residual proteins are denatured. Jung and co-workers demonstrated that β-lactoglobulin monomers heated at pH 2 for 5 h at 90 °C are more surface active than native monomers.[58] At very long times, further conformational rearrangements take place and a viscoelastic network is formed.[48–50] The formation of such network is confirmed by the dilatational frequency sweep after the 24 hours of adsorption. By analogy to the rheological behaviour of 3D-systems,[59] the interfacial protein films could behave as a viscoelastic liquid in the plateau regime or as a viscoelastic solid in the low frequency regime corresponding to the equilibrium modulus. Furthermore, this viscoelastic behaviour is observed at long time-scale suggesting a network structure which can be permanent or transitional. Whether the films behave as viscoelastic liquids or solids cannot be confirmed because of the reduced frequency range. However, all films are supramolecular large-scale networks that can be gels with strong bonds since the junction zones have relaxation times larger than 100 s.[59]

These kinetic and dilatational behaviours are different from the results obtained on aggregates produced after 24 hours of heat-treatment at 80 °C in a water bath.[54] These differences are to be related to the more rigid and cohesive long-heated aggregates that are mainly linked *via* disulfide bonds unlike these short-heated aggregates held mainly *via* hydrophobic bonds.[39] Davis and Foegeding found that heating WPI at 80 °C for 30 min resulted in a decrease in the adsorption rate and the dilatational properties[15] while Wang and Narsimhan found that the heat-induced denaturation (80 °C per 30 min) of β-lactoglobulin improves the adsorption rate at the air–water interface and results in a higher interfacial dilatational viscosity and a lower dilatational elasticity.[60] These contradictory results can be related to protein concentration (10% for WPI and 0.01 to 0.5% for β-lactoglobulin) which results in various residual fractions and especially various aggregate size and structure mainly held by covalent bonds.[56,61]

The enhancement of the surface activity upon heat treatment is then to be attributed to the dissociation of β-lactoglobulin dimers into monomers that occurs within seconds of heating above 60 °C, and to the denaturation of residual proteins, which results in an increased surface hydrophobicity and very likely in higher flexibility compared to native whey globular proteins.[31,32,56] The surface hydrophobicity controls the propensity of proteins to adsorb to the interface and the flexibility controls the partial unfolding upon adsorption increasing the residence time and the interactions with other proteins in the adsorbed layer.[4]

Spread monolayers

The conditions of concentration and ionic strength of protein solutions used in this study resulted in the formation of mixtures with very similar compositions at 80 °C: a large fraction (>65%) of residual proteins in monomeric form and a lower fraction of fractal aggregates. Whether they are spread in charge-screening or in long-range repulsion subphase conditions, monolayers of these mixtures show almost identical concentration regimes, viscoelasticity and structure. Indeed, the surface pressure shows a very clear power law dependence on the concentration. This behaviour is typical of flexible polymers in 2D, which implies that the proteins are at least partially unfolded at the interface. Additionally, the scaling exponents describing the power law dependence are larger than the values characteristic of native WPI. This difference is to be attributed to the fact that native WPI comprises mainly β-lactoglobulin dimers whereas heated WPI contains mainly β-lactoglobulin monomers. Indeed when heated above 60 °C, β-lactoglobulin dimers dissociate into monomers that collapse and have a more compact structure.[56] The scaling exponents found at high ionic strength, 8.3–8.5 for heated solutions and 7.1–7.5 for native WPI, are close from the scaling value for polymers in θ-solvent conditions, 8.[62,63] The values found at lower ionic strength, 6.2–6.3 for heated solutions and 5.5–5.7 for native WPI, are intermediate between an ideal (θ-conditions) chain and a chain in good solvent, 3.[62,63] A similar scaling value was found for β-lactoglobulin monolayer, 5.5, at

pH 7 and 0.02 M.[64] This change in scaling exponent corresponds to a swelling of the proteins due to non-screened surface charges. Apart from a more compact structure of protein film, heated WPI shows very similar spread monolayers where fractal aggregates, mainly linked together *via* hydrophobic interactions, disassembled into monomers and formed together with native-like monomers a homogeneous film. To confirm the importance of non-covalent bonds that stabilise fractal aggregates on their spreading behaviour, WPI solutions prepared at 80 °C in the plate heat-exchanger were further heated in thermostatted water bath at 80 °C for 15 to 120 min. Fig. 8A compares Π–A isotherms of WPI heated for 145 s at 80 °C in the plate heat-exchanger and further heated at the same temperature for 15 min. The isotherm shifted to higher concentrations and superimposes with isotherms heated for longer heating times (results not shown). This lower surface activity is to be mainly attributed to the covalent stabilisation of aggregates by disulfide bonds and then their increased cohesion (size of aggregates does not change).

In contrast to fractal aggregates, the spreading behaviour of spherical aggregates formed above 100 °C depends strongly on the ionic strength at which they are formed. Indeed, spherical aggregates formed at high ionic strength spread almost identically to fractal aggregates and native WPI in both charge-screening and long-range repulsion subphase conditions. This very similar spreading behaviour cannot result from the sole contribution of residual native-like proteins, but rather results from the dissociation of particles mainly into monomers and small aggregates as seen from AFM micrographs. These dissociated building units present a more compact structure in the monolayers than the native WPI when spread in charge-screening subphase conditions, the scaling exponent of power-law dependence of surface pressure on surface concentration in the dilute regime exceeding 8 (polymer chain in θ-conditions). When spread in subphase conditions of lateral long-range repulsion, they show the same scaling as native WPI, which implies that they are swollen due to surface charges that are not screened, and more unfolded than monomers that dissociated from fractal aggregates because the unfolding is more important above 100.[39,53] When formed at low ionic strength, spherical aggregates spread less than fractal aggregates and much less than native WPI, and the spreading weakens with increasing temperature. Additionally, they show granular films of 21–30 nm large objects (Fig. 11), which suggests that they dissociate into smaller cohesive aggregates when spread at the air–water interface. They become more surface active when spread in charge-screening subphase conditions but remain less surface active than native WPI especially at 120 °C. This weak surface spreading was confirmed by film elasticity where two low peaks are observed for the two subphase conditions. In some senses, this change in spreading behaviour can be linked to the internal structure of spherical aggregates, whose formation is determined by the magnitude of electrostatic repulsions. In the presence of salt, spherical aggregates have a fractal irregular internal structure with fractal dimension of 2.48, whereas in the absence of salt they have a more regular internal structure with fractal dimension of 1.3 (Fig. 3). Spherical aggregates with no-directional irregular internal structure completely dissociate at the air–water interface whereas spherical aggregates with essentially one-directional ordered internal structure dissociate only partially and above all into smaller aggregates that are weakly surface active. It is then the internal structure of aggregates that defines their dissociation and then their spreading at the air–water interface.

For almost all the aggregates and native proteins investigated in this study, the monolayer elasticity shows two close peaks when spread in long-range repulsion subphase conditions and a single peak followed by a shoulder when spread in charge-screening subphase conditions. Very similar results were found for long-heated fractal aggregates. While the first maximum is generally associated with a conformational change in the protein monolayer,[26] the second peak could be related to charge anisotropy that induces reorientation of molecules when compressed and then promotes electrostatic attractions between opposite charges.[54]

Conclusions

The differences observed in the effect of heat treatment on spreading and adsorption behaviours can be attributed to the non-limiting concentration used in adsorption experiments. The denatured non-aggregated monomers adsorb first at the air–water interface and form films that are strengthened by the rearrangements and the formation of strong interactions between the adsorbed molecules. This is in contrast to spreading experiments where the amount spread at the air–water interface corresponds to the quantity classically used for whey proteins to form a monolayer. This allowed understanding the behaviour of aggregates at the air–water interface and their ability to form elastic monolayers. Their behaviour is strongly dependent on their internal structure and on the electrostatic interactions but cannot be correlated to the heat-induced changes of secondary structure.

Acknowledgements

The authors thank Michèle Dalgalarrondo, Geneviève Llamas, Cédric Gaillard, François Boué, Patrick Gunning and Taco Nicolai for help with experiments and useful discussions. N.M. acknowledges the Région Pays de la Loire for funding through VANAM project.

References

1 P. J. Wilde, *Curr. Opin. Colloid Interface Sci.*, 2000, **5**, 176–181.
2 S. Damodaran, *J. Food Sci.*, 2005, **70**, 54–66.
3 R. D. Waniska and J. E. Kinsella, *J. Agric. Food Chem.*, 1985, **33**, 1143–1148.
4 M. Cornec, D. Cho and G. Narsimhan, *J. Colloid Interface Sci.*, 1999, **214**, 129–142.
5 D. E. Graham and M. C. Phillips, *J. Colloid Interface Sci.*, 1979, **70**, 403–414.
6 P. Suttiprasit, V. Krisdhasima and J. McGuire, *J. Colloid Interface Sci.*, 1992, **154**, 316–326.
7 E. Dickinson, *J. Chem. Soc., Faraday Trans.*, 1992, **88**, 2973–2983.
8 E. Dickinson, *J. Chem. Soc., Faraday Trans.*, 1998, **94**, 1657–1669.
9 A. H. Martin, K. Grolle, M. A. Bos, M. A. Cohen Stuart and T. van Vliet, *J. Colloid Interface Sci.*, 2002, **154**, 175–183.
10 S. Sourdet, P. Relkin and B. Cesar, *Colloids Surf., B*, 2003, **31**, 55–64.
11 M. Mellema and J. G. Isenbart, *J. Dairy Sci.*, 2004, **87**, 2769–2778.
12 C. Holt, D. McPhail, T. Nylander, J. Otte, R. H. Ipsen, R. Bauer, L. Ogendal, K. Olieman, K. G. Kruif, J. Leonil, D. Molle, G. Henry, J. L. Maubois, M. D. Perez, P. Puyol, M. Calvo, S. M. Bury, G. Kontopidis, L. McNae, L. Sawyer, L. Ragona,

L. Zetta, H. Molinari and B. Klarenbeek, *Int. J. Food Sci. Technol.*, 1999, **34**, 587–601.
13 C. V. Morr and E. Y. W. Ha, *Crit. Rev. Food Sci. Nutr.*, 1993, **33**, 431–476.
14 M. A. de la Fuente, Y. Hemar, M. Tamehana, P. A. Munro and H. Singh, *Int. Dairy J.*, 2002, **12**, 361–369.
15 J. P. Davis and E. A. Foegeding, *J. Food Sci.*, 2004, **69**, C404–C410.
16 F. MacRitchie and A. E. Alexander, *J. Colloid Sci.*, 1963, **18**, 464–469.
17 M. Blank, B. B. Lee and J. S. Britten, *J. Colloid Interface Sci.*, 1975, **50**, 215–222.
18 J. P. Davis, E. A. Foegeding and F. K. Hansen, *Colloids Surf., B*, 2004, **34**, 13–23.
19 D. Cho, G. Narsimhan and E. I. Franses, *J. Colloid Interface Sci.*, 1997, **191**, 312–325.
20 S. Hambling, A. S. McAlpine and L. Sawyer, in *Advanced Dairy Chemistry Volume1: Proteins*, ed. P. F. Fox, Elsevier Applied Science, London, 1992, vol. 1, pp. 141–190.
21 E. A. Permyakov and L. J. Berliner, *FEBS Lett.*, 2000, **473**, 269–274.
22 K. Kuwajima, *FASEB J.*, 1996, **10**, 102–109.
23 K. B. Song and S. Damodaran, *Langmuir*, 1991, **7**, 2737–2742.
24 P. A. Wierenga, M. B. J. Meinders, M. R. Egmond, A. G. J. Voragen and H. H. J. deJongh, *J. Phys. Chem. B*, 2005, **109**, 16946–16952.
25 J. R. Lu, T. J. Su and B. J. Howlin, *J. Phys. Chem. B*, 1999, **103**, 5903–5909.
26 D. E. Graham and M. C. Phillips, *J. Colloid Interface Sci.*, 1979, **70**, 415–426.
27 D. E. Graham and M. C. Phillips, *J. Colloid Interface Sci.*, 1979, **70**, 427–439.
28 P. Cicuta, *J. Colloid Interface Sci.*, 2007, **308**, 93–99.
29 P. J. Atkinson, E. Dickinson, D. S. Horne and R. M. Richardson, *J. Chem. Soc., Faraday Trans.*, 1995, **91**, 2847–2854.
30 J. M. Rodrýguez Patino, M. R. Rodrýguez Niño, C. Carrera Sanchez, J. M. Navarro Garcýa, G. Rodrýguez Rodrýguez Mateo and M. Cejudo Fernandez, *Colloids Surf., B*, 2001, **21**, 87–99.
31 R. Wijesinha-Bettoni, C. Gao, J. A. Jenkins, A. R. Mackie, P. J. Wilde, E. N. C. Mills and L. J. Smith, *Biochemistry*, 2007, **46**, 9774–9784.
32 D. A. Kim, M. Cornec and G. Narsimhan, *J. Colloid Interface Sci.*, 2005, **285**, 100–109.
33 L. P. Voutsinas, E. Cheung and S. Nakai, *J. Food Sci.*, 1983, **48**, 26–32.
34 A. Kato, Y. Osako, N. Matsudomi and K. Kobayashi, *Agric. Biol. Chem.*, 1983, **47**, 33–37.
35 J. S. Higgins and H. C. Benoît, *Polymers and Neutron Scattering*, Clarendon Press, Oxford, 1993.
36 P. Stepanek, in *Dynamic Light Scattering*, ed. W. Brown, Oxford University Press, Oxford, 1993, pp. 177–241.
37 P. Calmettes, *J. Phys. IV*, 1999, **9**, 83–93.
38 J. P. Cotton, *J. Phys. IV*, 1999, **9**, 21–49.
39 N. Mahmoudi, C. Gaillard, A. Riaublanc, F. Boué and M. A. V. Axelos, *Eur. Phys. J. E*, 2011, submitted.
40 J. Benjamins, A. Cagna and E. H. Lucassen-Reynders, *Colloids Surf., A*, 1996, **114**, 245–254.
41 P. Cayot and D. Lorient, *Structures et technofonctions des protéines du lait*, Lavoisier TEC&DOC, Paris, 1998.
42 T. Hendrix, Y. V. Griko and P. L. Privalov, *Biophys. Chem.*, 2000, **84**, 27–34.
43 J. C. Gimel, D. Durand and T. Nicolai, *Macromolecules*, 1994, **27**, 583–589.
44 P. Aymard, D. Durand and T. Nicolai, *Int. J. Biol. Macromol.*, 1996, **19**, 213–221.
45 M. Kataoka, K. Kuwajima, F. Tokunaga and Y. Goto, *Protein Sci.*, 1997, **6**, 422–430.
46 M. L. Ferrer, R. Duchowicz, B. Carrasco, J. G. de la Torre and A. U. Acuña, *Biophys. J.*, 2001, **80**, 2422–2430.
47 W. C. K. Poon and M. D. Haw, *Adv. Colloid Interface Sci.*, 1997, **73**, 71–126.
48 C. J. Beverung, C. J. Radke and H. W. Blanch, *Biophys. Chem.*, 1999, **81**, 59–80.
49 B. C. Tripp, J. J. Magda and J. D. Andrade, *J. Colloid Interface Sci.*, 1995, **173**, 16–27.
50 E. M. Freer, K. S. Yim, G. G. Fuller and C. J. Radke, *J. Phys. Chem. B*, 2004, **108**, 3835–3844.
51 L. G. C. Pereira, O. Theodoly, H. W. Blanch and C. J. Radke, *Langmuir*, 2003, **19**, 2349–2356.
52 R. A. L. Jones and R. W. Richards, in *Polymers at Surfaces and Interfaces*, C.U. Press, Cambridge, 1999.
53 P. Cicuta and I. Hopkinson, *J. Chem. Phys.*, 2001, **114**, 8659–8670.
54 N. Mahmoudi, C. Gaillard, F. Boué, M. A. V. Axelos and A. Riaublanc, *J. Colloid Interface Sci.*, 2010, **345**, 54–63.
55 A. R. Mackie, A. P. Gunning, P. J. Wilde and V. J. Morris, in *Food Colloids Fundamentals of Formulation*, ed. E. Dickinson and R. Miller, The Royal Society of Chemistry, Cambridge, 2001, pp. 13–21.
56 S. Cairoli, S. Iametti and F. Bonomi, *J. Protein Chem.*, 1994, **13**, 347–354.
57 D. Renard, PhD thesis, Université de Nantes, 1994.
58 J.-M. Jung, D. Z. Gunes and R. Mezzenga, *Langmuir*, 2010, **26**, 15366–15375.
59 J. D. Ferry, *Viscoelastic Properties of Polymers*, John Wiley &Sons, Inc., New York, 3rd edn, 1980.
60 Z. Wang and G. Narsimhan, *Langmuir*, 2005, **21**, 4482–4489.
61 C. Schmitt, C. Moitzi, C. Bovay, M. Rouvet, L. Bovetto, L. Donato, M. E. Leser, P. Schurtenberger and A. Stradner, *Soft Matter*, 2010, **6**, 4876–4884.
62 M. Daoud and P. G. Degennes, *J. Phys.*, 1977, **38**, 85–93.
63 M. Daoud and G. Jannink, *J. Phys.*, 1976, **37**, 973–979.
64 P. Cicuta and E. M. Terentjev, *Eur. Phys. J. E*, 2005, **16**, 147–158.